



HAL
open science

Direct Electrografting of Poly(2-alkyl-2-oxazoline)s on Gold, ITO, and Gold Nanoparticles for Biopassivation

Dihia Benaoudia, Van-Quynh Nguyen, Véronique Bennevault, Pascal Martin, Fabien Montel, Philippe Guégan, Jean-Christophe Lacroix

► **To cite this version:**

Dihia Benaoudia, Van-Quynh Nguyen, Véronique Bennevault, Pascal Martin, Fabien Montel, et al.. Direct Electrografting of Poly(2-alkyl-2-oxazoline)s on Gold, ITO, and Gold Nanoparticles for Biopassivation. ACS Applied Nano Materials, 2023, 6 (18), pp.16267-16275. 10.1021/acsnm.3c02379 . hal-04219821

HAL Id: hal-04219821

<https://cnrs.hal.science/hal-04219821>

Submitted on 27 Sep 2023

HAL is a multi-disciplinary open access archive for the deposit and dissemination of scientific research documents, whether they are published or not. The documents may come from teaching and research institutions in France or abroad, or from public or private research centers.

L'archive ouverte pluridisciplinaire **HAL**, est destinée au dépôt et à la diffusion de documents scientifiques de niveau recherche, publiés ou non, émanant des établissements d'enseignement et de recherche français ou étrangers, des laboratoires publics ou privés.

This document is confidential and is proprietary to the American Chemical Society and its authors. Do not copy or disclose without written permission. If you have received this item in error, notify the sender and delete all copies.

**Synthesis and Direct Electrografting of Poly(2-oxazoline)s
on Gold, ITO and Gold Nanoparticule Surfaces for
Biopassivation.**

Journal:	<i>ACS Applied Nano Materials</i>
Manuscript ID	Draft
Manuscript Type:	Article
Date Submitted by the Author:	n/a
Complete List of Authors:	Benaoudia, Dihia; Universite Paris Diderot, ITODYS; UPMC, Institut Parisien de Chimie Moléculaire (IPCM) - UMR 8232 Chimie des Polymères Nguyen, Van Quynh; Hanoi University of Science and Technology, Advanced Materials Science and Nanotechnology Bennevault, Véronique; IPCM Martin, Pascal; Universite Paris Diderot, Chemistry Montel, Fabien; Laboratoire de Physique de l'ENS de Lyon, Guegan, Philippe; UPMC, Institut Parisien de Chimie Moléculaire (IPCM) - UMR 8232 Chimie des Polymères Lacroix, Jean-Christophe; Universite Paris Diderot, ITODYS

SCHOLARONE™
Manuscripts

Synthesis and Direct Electrografting of Poly(2-oxazoline)s on Gold, ITO and Gold Nanoparticle Surfaces for Biopassivation.

Dihia Benaoudia^{1,2}, Van-Quynh Nguyen^{1,3}, Véronique Bennevault^{2,4}, Pascal Martin¹, Fabien Montel⁵, Philippe Guégan*², Jean-Christophe Lacroix*¹.

¹Université Paris Cité, ITODYS, UMR 7086 CNRS, 15 rue Jean-Antoine de Baïf, 75205 Paris Cedex 13, France

²Institut Parisien de Chimie Moléculaire, Equipe Chimie des Polymères, Sorbonne Université, CNRS, 4 place Jussieu, 75005 Paris, France

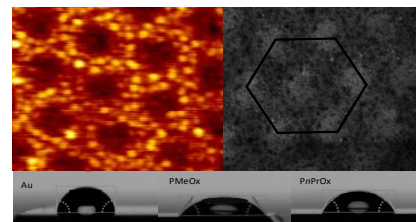
³Department of Advanced Materials Science and Nanotechnology, University of Science and Technology of Hanoi (USTH), Vietnam Academy of Science and Technology, 18 Hoang Quoc Viet, 11307 Cau Gay, Hanoi Vietnam;

⁴University of Evry, Rue du Père Jarlan, 91025 Evry Cedex, France

⁵Univ Lyon, ENS de Lyon, CNRS, Laboratoire de Physique, F-69342 Lyon, France

KEYWORDS: surface functionalization, cationic ring-opening polymerization, diazonium salt reduction, poly(2-oxazoline)s, smart surface

ABSTRACT: Poly(2-oxazoline)s (POx) bearing an aminophenyl end group were synthesized by cationic ring-opening polymerization, the polymers were then carefully characterized by NMR, size exclusion chromatography and differential scanning nano calorimetry. The electroreduction of the diazonium salts of aniline terminated poly(2-methyl-2-oxazoline) (PMeOx) and poly(2-*n*-propyl-2-oxazoline) (PnPrOx) from aqueous solution on indium tin oxide (ITO), gold (Au) and through a two-dimensional poly(styrene) (PS) template has been investigated. On all substrates, ultrathin layers of polymer are grafted and deposited. Modified surfaces were characterized by electrochemistry, scanning electron microscopy (SEM), X-ray photoelectron spectroscopy (XPS) and atomic force microscopy. Nanoporous honeycomb POx structures have been obtained thanks to the electrochemical growth in the interstitial spaces between self-assembled PS spheres. Finally, the wettability of the surfaces depends markedly on the chemical nature of the POx, with contact angles of 32° and 70° for modified surfaces with PMeOx and PnPrOx.



INTRODUCTION

Surface modification has been widely addressed in corrosion protection^{1,2,3} smart coatings,^{4,5,6,7} sensing and biomedical applications.^{8,9,10} Adsorption of thiol-organic compounds onto a gold surface was revealed to be an easy strategy to form self-assembled monolayers that could be the base for further building more complex structures^{11,12} This easy process is however hampered by the poor stability of such layers in harsh conditions, especially in oxidative or reductive media¹³ In the case of SiO₂ surface, the silane chemistry is the most common process used.^{14,15} Both chemistries have been extended to other metal and oxide surfaces modifications. Grafting a poly(aryl) based layer using diazonium salts reduction is another strategy that could be used for surface modification of many substrates (metallic, semi-conducting, polymer, diamond, carbon nanotubes ...) ^{16,17,18} This grafting chemistry relies on the formation of aryl radical from diazophenyl derivatives, able then to react with any surface. Formation of the aryl radical was firstly ensured by electroreduction^{16,17} but it was later shown that ultrason, UV and visible light could also be used to generate the reactive phenyl radical.^{19,20,21} This grafting

chemistry offers an ease of preparation, a large choice of available reactive functional group and a strong aryl-surface bonding. The structure of the aryl film can however be complex: the reactive aryl radical reacts on the surface, but also on the first grafted aryl residues. The resulting organic layer is then composed of many aryl layers with total film thickness ranging from few nm, when the deposited film is insulating, ^{22,23,24} to μm when it incorporates redox active groups acting as electronic relay during electrochemical reduction.^{25,26,27} Several strategies have been proposed to limit the growth of multilayers. Among them, the use of sterically hindered aryl derivatives such as 3,5-bis-*tert*-butyl benzenediazonium salts²⁸, of diazonium salts derived from inorganic complexes^{29,30} or bearing bulky protective groups³¹, the use of ionic liquids³² or of radical scavengers.^{33,34,35}

Grafting saturated polymers on surfaces is an important coating strategy for protective issue of the surface, antifouling properties, controlled wettability, chelating surfaces, molecular imprinted polymer grafts, to name but a few of the most frequent targeted properties. ^{36,37,38} Polymer chemisorption, i.e. the grafting of a polymer chain on a surface via a covalent bond, has been found to be more

resistant than physisorption and the grafting can be ensured via various strategies: a “grafting from” strategy consisting of a polymerization of a monomer from a small initiator already grafted on the surface, or a “grafting onto” method issued from the grafting of a premade polymer onto a surface via a chemical reaction. The “grafting from” method requires an efficient initiation reaction with a fast kinetic of the propagating step that essentially limits the polymer “grafting from” approach to radical chemistry. In this respect, most of the work dedicated to formation of polymeric monolayer on a surface using the diazonium salt chemistry relies on building a first functional aryl layer on which initiation functions are grafted to start the growing of polymer chains from the surface.³⁹ Grafting brominated aryl layers on surfaces enabled the use of atom transfer radical polymerization to control the molar mass of the grafted polymer layers and to provide very dense polymer layers.^{40,41} This grafting strategy was for example applied to methacrylate, N-isopropylacrylamide, vinylpyridine or styrene monomers⁴². Homopolymer grafts from R-tert-butoxy- ω -vinylbenzyl-polyglycidol (PGL) were prepared on gold and stainless steel substrates modified by 4-benzoyl-phenyl moieties derived from the electroreduction of the parent salt 4-benzoylbenzene diazonium tetrafluoroborate.

Grafting onto is an alternative strategy in which a first aryl layer bearing various coupling groups is deposited on a surface and a premade polymer is attached on this layer in a second step. Several examples can be found in the literature. The attachment of carboxyphenyl groups to the iron surface by reduction of the diazonium salt of 4-aminobenzoic acid and the further attachment of poly(1,2-propanediyl fumarate) to the phenylcarboxylate functions through ionic bonds with Mg²⁺ ions was reported thirty years ago.⁴³ *clicking* macromolecules to grafted, diazonium salt-derived aryl layers was shown to be a simple and valuable approach for designing robust, functional surface organic coatings.⁴⁴ Grafting long PEG oligomers or commercial surfactants by a reaction of the linear polymer with a premade aryl layer was recently reported.⁴⁵ Functional polymers bearing diazonium terminal group have also been synthesized, and then grafted onto the surface. Low molar masses oligomers of tetra(ethylene oxide) derivatives have been used with this coupling chemistry⁴⁶ in order to generate surface modulation of single-walled carbon nanotubes for selective bacterial cell agglutination.

Polypyrrolidone, polyglycidol or polyoxazoline have recently be proposed to replace PEG for various reasons ranging from better fouling properties⁴⁷ to higher biocompatibility.⁴⁸ Polyoxazoline was recently widely developed for biological applications, and revealed a high potential for PEG substitution in every application related to medical science and surface coating.⁴⁹

Grafting from polymerization of 2-ethyl-2-oxazoline on a surface was reported by Jordan *et al.* as early as 1998^{50,51}. The initiator was first linked to the surface using the thiol-gold chemistry, then a grafting from polymerization of 2-ethyl-2-oxazoline was conducted to provide a polymer monolayer with a high estimated grafting density. Linear or cyclic polyoxazolines were grafted onto surfaces using thiol chemistry^{52,53} or polyelectrostatic interactions.⁵⁴

Quite large molar masses of polyoxazoline could be grafted on various surfaces, however, the long-term robustness of the anchoring could be questioned. Surprisingly, the grafting of polyoxazoline from polymers bearing diazonium end groups has never been reported, while this versatile strategy represents an original way to coat any surface by polymers through robust aryl covalent anchor.

In the present work we will first describe the one-pot synthesis of aniline end-functionalized polyoxazolines, thanks to a controlled termination reaction between 1-(4-aminophenyl)piperazine and the oxazolinium function of the growing polyoxazoline chains. This reaction will be investigated for two series of oxazoline monomers, i.e. 2-methyl-2-oxazoline (MeOx) and 2-*n*-propyl-2-oxazoline (*n*-PrOx). Then grafting of the polymers on a gold surface using the electro-reduction of *in situ* formed diazonium reactive functions from the terminal aminophenyl groups born by the polymers with various molar masses was studied. The effect of the LCST of the poly(2-*n*-propyl-2-oxazoline) onto the grafted polymer layer will be investigated.

RESULTS AND DISCUSSION

Synthesis of PMeOx and P*n*PrOx

Oxazoline monomers were polymerized in acetonitrile at 80°C, conditions that were reported to provide controlled polymerizations.^{55,56} Allyl bromide was selected as initiator in order to enable a fast and complete initiation reaction (Figure 1). For all the experiments, targeted degrees of polymerization (X_n), calculated from initial molar concentrations ratio $[M]_0/[A]_0$ (i.e., assuming quantitative initiation), were deliberately set between 30 and 60. So chain ends could be easily characterized by ¹H NMR for the termination reaction investigation. 1-(4-aminophenyl)piperazine was selected as the quencher to provide polyoxazolines with aminophenyl chain-ends. Assumption was made the secondary amino function of the piperazine derivative would react much faster than the aniline function with the oxazolinium growing chain ends.

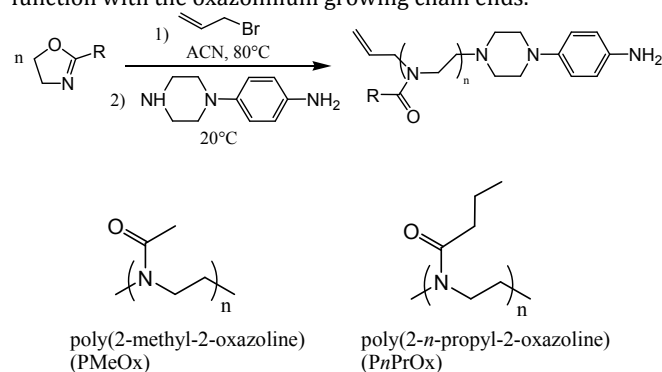


Figure 1. Cationic Ring-Opening Polymerization of 2-alkyl-2-oxazolines (MeOx or *n*-PrOx)

First polymerizations of MeOx were conducted for 24 hours at 80°C (Table 1) and the quenching time by 1-(4-aminophenyl)piperazine was set to 66 hours, with a quencher/initiator ratio between 1.2 and 5. NMR analyses of the reaction media revealed a complete monomer conversion within the 24h. Using the unsaturation signal at 5.23 ppm witnessing the allyl end chains and the monomer unit signal at 3.44 ppm, the NMR degrees of polymerization were determined on the purified

polymers spectra. The functionality of the polymers was calculated comparing the intensity of the piperazine cycle methylene protons at 3.05 ppm and 2.66 ppm and the intensity of the unsaturated protons at 5.80 ppm. In our first trial, the conditions used (1.2 eq. of quencher / initiator) led to only 46% of functionalization by the aminophenyl group (run 1), while a quencher/initiator ratio equal to 5 enabled to obtain a functionality equal to 79% (run 2). Probably a quencher excess higher than 5 would enable to obtain a quantitative functionalization. Nevertheless, this rate is sufficient for the targeted application, since after the grafting step, the surface was washed, suppressing the non functionalized chains. The chemical structure of the synthesized polymers was confirmed by 1D (Figure 2) and 2D NMR analyses (COSY, HSQC and DOSY NMR, Figures S1 to S3). The DOSY experiments showed the covalent bond between the polymer and the piperazine derivative, since all the NMR signals broadcasted at the same speed. The polymers had diffusion coefficients (Table 1) in the

range of $2.10 \cdot 10^{-10} \text{ m}^2 \cdot \text{s}^{-1}$ that was much lower than the value determined in the same conditions for 1-(4-aminophenyl)piperazine. The latter was equal to $(1.34 \pm 0.01) \cdot 10^{-9} \text{ m}^2 \cdot \text{s}^{-1}$. The functionalization of the chains was also highlighted by Size Exclusion Chromatography (SEC), since an overlap of the RI and UV signals was observed (Figure S4). This result indicated that all the chains contained a piperazine group. However, the SEC chromatograms showed a shoulder towards high elution volume, whose intensity increased with decreasing quencher/initiator ratio. The molar mass of this population was twice as high as the main population one. These results suggest that a small fraction of growing chains is deactivated both by the piperazine and aniline end chains of 1-(4-aminophenyl)piperazine. Note that these chains are eliminated during the washing of the grafted surface. This issue is solved by increasing the excess of quencher. With an excess of 5 (Table 1, run 2), the degrees of polymerization determined by SEC and NMR are in good agreement with the theoretical value.

Run ^a	$[M]_0/[A]_0/[Q]_0$ ^b	Conv ^c (%)	$X_{n,th}$ ^d	$X_{n,NMR}$ ^e	$X_{n,SEC}$ ^f	\bar{D} ^f	F ^g (%)	Diff. Coef ^h ($\text{m}^2 \cdot \text{s}^{-1}$)
1	60/1/1.2	98	58	95	81	1.26	46	$(2.2 \pm 0.1) \cdot 10^{-10}$
2	55/1/5	99	54	66	64	1.25	79	$(2.0 \pm 0.1) \cdot 10^{-10}$

^aSolvent : ACN, Temperature: 80°C, Quench time: 66h, ^b $[A]_0$, $[M]_0$, $[Q]_0$: respectively initial initiator, monomer and quencher concentration, $[M]_0 = 1.5 \text{ mol} \cdot \text{L}^{-1}$, ^cMonomer conversion determined from the medium reaction by ¹H NMR in CDCl_3 , ^d $X_{n,th} = [M]_0 \times \text{Conv} / [A]_0$, ^eDetermined by ¹H NMR from allyl end chains, ^fDetermined by SEC (DMF, 60°C, PMMA standards), ^gfonctionnalization ratio determined by ¹H NMR, ^hDiffusion coefficient determined by DOSY NMR.

Table 1 : Experimental Conditions and Molecular Characteristics of PMeOX

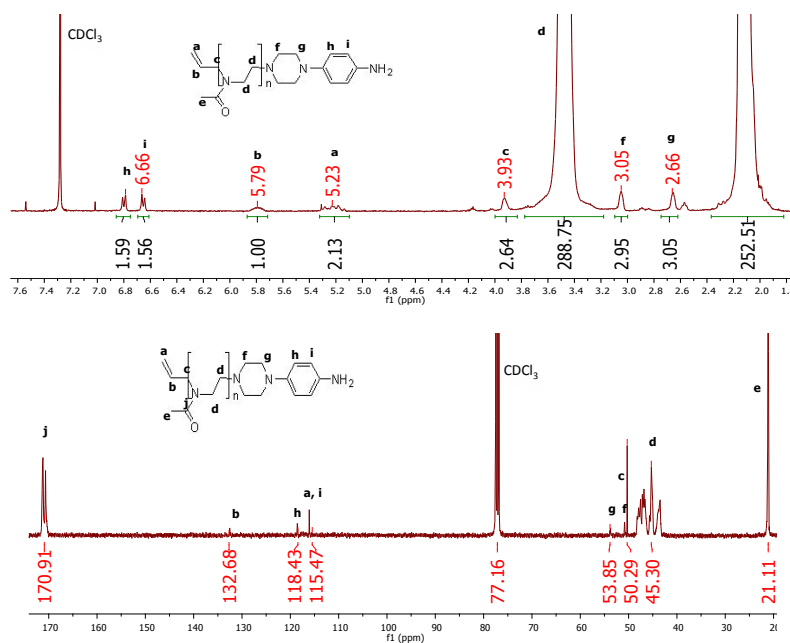


Figure 2 : ¹H and ¹³C NMR of PMeOX (Table 1, run 2) recorded in CDCl_3 at 20°C.

A ratio $[Q]_0/[A]_0$ equal to 5 was then used to synthesize poly(2-*n*-propyl-2-oxazoline)s (P*n*PrOx). Data are collected in Table 2. The structure of the polymers was confirmed by NMR (Figure 3A and Figures S5-S6). Once again, the covalent bond between the polymer chain and the quencher was highlighted by SEC (Figure 3B) and by the measurement of the diffusion coefficients by DOSY NMR (Figure 3C). In this set of experiments, an excess of quencher equal to 5 was sufficient to obtain a complete functionalization of the chains during the termination step and no shoulder was observed in the SEC chromatograms, suggesting a high control of the polymers structure. This point is in agreement with the lower dispersities and the lower standard deviations of diffusion coefficients respectively obtained in

SEC and NMR (Table 2). This kind of polymers is known to have a lower critical solution temperature (LCST). The LCST values determined by nanoDSC are about 25°C ($[PnPrOx] = 5$ mg/mL). A small variation was noted according to the polymerization degree of the sample ($X_{n, SEC} = 38$ or 64). The values obtained in this study are close to the published values.^{57,58} For example, a LCST of 30°C was mentioned for a polymer with methyl and alcohol end-chains and with a X_n equal to 60.⁵⁷ The more hydrophobic aminophenyl group induced a slight decrease of the LCST value in the present case.

Run ^a	$[M]_0/[A]_0/[Q]_0$ ^b	t_{polym} ^c (h)	Conv ^d (%)	$X_{n, th}$ ^e	$X_{n, NMR}$ ^f	$X_{n, SEC}$ ^g	\bar{D} ^g	F ^h (%)	Diff. Coef ⁱ (m ² .s ⁻¹)	LCST (°C)
3	32/1/5	24	94	30	48	64	1.06	95	$(1.94 \pm 0.04) \cdot 10^{-10}$	23
4	40/1/5	48	98	39	40	38	1.10	100	$(2.42 \pm 0.06) \cdot 10^{-10}$	26

^aSolvent: ACN, Temperature: 80°C, Quench time: 66h, ^b $[A]_0$, $[M]_0$, $[Q]_0$: respectively initial initiator, monomer and quencher concentration, $[M]_0 = 1.5$ mol.L⁻¹,

^cpolymerization time, ^dMonomer conversion determined from the medium reaction by ¹H NMR in CDCl₃, ^e $X_{n, th} = [M]_0 \times Conv / [A]_0$, ^fDetermined by ¹H NMR from allyl end chains, ^gDetermined by SEC (DMF, 60°C, PMMA standards), ^hfunctionalization ratio determined by ¹H NMR, ⁱDiffusion coefficient determined by DOSY NMR.

Table 2 Experimental Conditions and Molecular Characteristics of P*n*PrOx

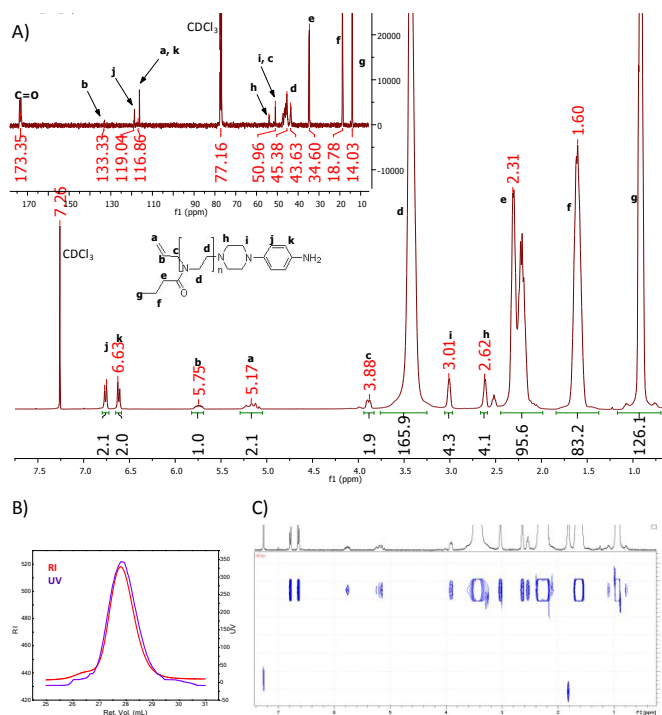


Figure 3: P*n*PrOX (Table 2, run 4): A) ¹H and ¹³C NMR in CDCl₃ at 20°C; B) SEC trace: RI (red), UV (purple) at $\lambda = 254$ nm; C) DOSY NMR in CDCl₃ at 298 K

Electrografting:

PMeOx was grafted by the electrochemical reduction of diazonium salts on various electrodes (Gold, ITO, ITO bearing gold nanotriangles). As an example, Figure 4 shows the electrochemical grafting performed in acetonitrile by cyclic voltammetry. The diazonium salt was generated *in situ* from PMeOx-aminophenyl in the presence of $t\text{BuNO}_2$. The recorded CV displays irreversible reduction waves at -0.09 V and a broad reduction current from 0.3 to -0.8 V , associated with the reduction of PMeOx diazonium. During subsequent cycles, the intensity of the cathodic current decreases. Similar behavior has been observed during the reduction of *in situ* generated aryldiazonium cations.⁵⁹ This behavior is attributed to the progressive modification of the electrode by the formation of an insulating organic film, which partially blocks the surface in the 0.45 to -0.8 V potential range. The electrochemical reduction of the other polymers $Pn\text{PrOx}$, behaves similarly,

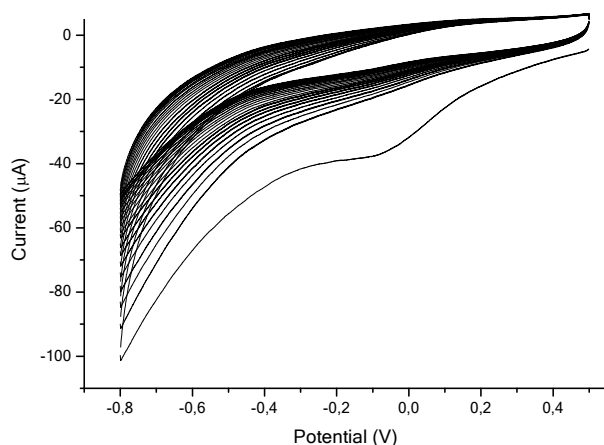


Figure 4 Cyclic voltammogram of PMeOx electrografting by electroreduction of the associated diazonium ($5 \times 10^{-4}\text{ M}$ in ACN with 20 eq of $t\text{BuNO}_2$ and 0.1 M of TBAPF_6 on ITO electrode Scan rate 0.1 V/s

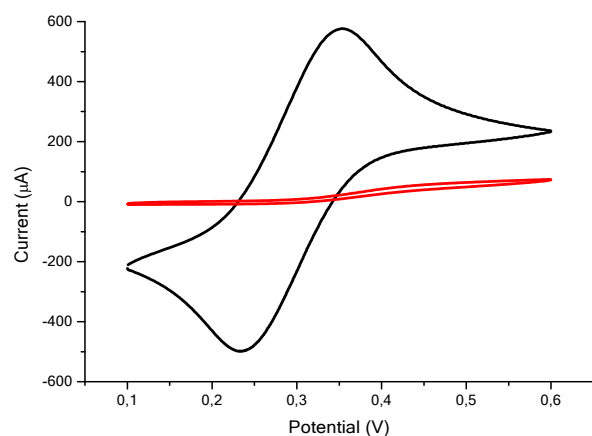


Figure 5 CVs of ferrocene (10^{-3} M in acetonitrile with 0.1 M LiClO_4) at 100 mVs^{-1} before (black line) and after grafting of PMeOx on ITO electrode

The blocking effect of the deposited layer was investigated using redox probes in solution. The voltammogram of Ferrocene (Fc) in ACN solution on ITO electrode was recorded (Figure 5) before (black) and after (red) PMeOx electrografting. A strong decrease of the current of ferrocene is observed on the modified ITO electrode. This confirms that a compact film has been deposited on all the ITO surface which is covered by the polymer.

XPS analysis was also used to analyze the surface composition of the generated film. To do so, we deposited the various films on a 1 cm^2 gold electrode.

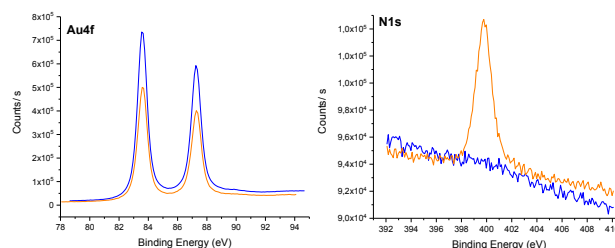


Figure 6 High-resolution XPS spectra of a gold surface, before (blue) and after (orange) polymer electrografting. a) high resolution Au_{4f} signals, b) high resolution N_{1s} signal

Figure 6 displays the high-resolution XPS signal for Au_{4f} (peaks, around, 84 and 88 eV Figure 6a) and the high-resolution XPS signal for N_{1s} (peak around 400 eV Figure 6b) obtained on the Au modified surface. Several major differences can be observed in the XPS spectra before and after electrochemical grafting. First, the gold signal decreases with the bare substrate, which indicates the formation of an organic layer. Second, the detection of the Au XPS signals, in the survey spectrum is an indication of rather thin film, below 10 nm . Third a nitrogen signal appears after polymer deposition.

Ratio	theoretical	experimental
O/N	0.96	0.94
O/C	0.05	0.03
N/C	0.17	0.15

Table 3 Summary of XPS results

Table 3 summarizes the experimental and theoretical ratios of the different elements observed on the grafted surface. The ratio O/N found by XPS analysis (0.94) is in very good agreement with the theoretical composition of the PMeOx if immobilized on the surface (0.96). N/C and O/C ratios are also in very good agreement with theoretical ratios which confirms that a thin film of PMeOx is grafted on the gold surface.

Measuring the thickness of such film is not easy and was done, in this study using nanosphere lithography combined with PMeOx diazonium salt electroreduction.^{23,29,60} A monolayer of PS spheres (500 nm diameter) was first deposited on a ITO surface using an already published procedure.⁶¹ PMeOx diazonium salt electroreduction was then performed on these nanostructured electrodes and grafting confined in the free

space between adjacent nanospheres. PS Spheres were then removed in THF under ultrasonic conditions and the generated surface was studied by SEM and AFM. **Figure 7** shows that the surface consists of nano-hole array hexagonally organized on a large area. Indeed, after the removal of the spheres, the SEM image shows white circular spots, organized in a honeycomb arrangement, within dark areas. The apparent diameter of each white spot is 200 nm, corresponding to the area previously occupied by the PS spheres. The center-to-center distance between two adjacent circular spots is 500 nm and corresponds to the diameter of the spheres used. This clearly confirms that the spheres are close-packed, with an organized 2D layer acting as a mask for diazonium electroreduction. The surfaces after bead dissolution consist clearly of a hexagonal organization of nanometric holes in a layer of grafted poly(2-methyl-2-oxazoline)s. Free ITO areas are clearly visualized as white spots in the SEM image of the modified surface.

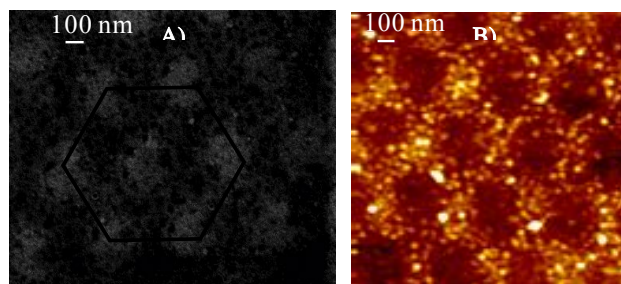


Figure 7 A) SEM image. B) AFM image of nano structured array of e Polyoxazoline layer on ITO obtained using 500 nm diameter PS sphere

The topology and morphology of the nanostructure on the ITO surface was further characterized by AFM (**Figure 7B**). Holes in the PMeOx layer are now seen as dark spots and the honeycomb arrangement in nano-hole arrays is clearly observed. The AFM topographies exhibit brighter areas where PMeOx grafting took place and show a local morphology with small protuberance likely indicating that the grafted polymer self-aggregates which yields to a high local roughness when compared to similar surface deposited from diazonium grafting using smaller molecules.^{23,29} **Figure 8** shows an AFM image of a larger area along with the line profile. It shows an average hole height between 3 and 5 nm and confirms that the PMeox film is ultrathin and that due to the steric hindrance of the long polymer chains, thick multilayers are not obtained. Note also that thicknesses measured by AFM are coherent with those deduced from Au XPS signal.

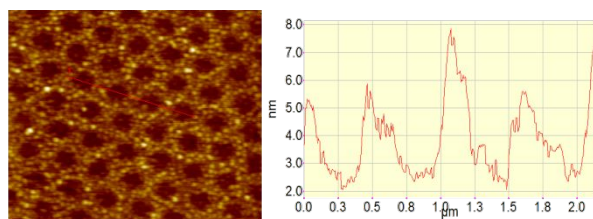


Figure 8 A) AFM images. B) line profile along the red line of the PMeOx nano structured layer on ITO obtained using nanosphere lithography (500 nm diameter PS sphere)

Next, the contact angles of water on various PMeOx and PnPrOx modified gold electrodes, generated by cyclic voltammetry were measured and compared. Films generated from PMeOx-aminophenyle, run 1 and run 2 (**Table 1**), in the presence of tBuNO₂ in AcN are characterized by water contact angle of 32° and 55° respectively, i.e. smaller than the 83° contact angle measured on the Au bare surface. PMeOx modified surfaces are thus more hydrophilic than bare gold because of the hydrosoluble properties of the grafted polymer and increasing the chain length (between run 1 and run 2) decreases the contact angle. On PnPrOx-Au modified surface the contact angle reaches 70° (**Figure 9**). These results are in good agreement with the chemical properties of polyoxazolines as it is known that PnPrOx is less hydrophilic than PMeOx. Overall, the variations of the contact angles after the electrografting process indicate that the hydrophilic polymers are grafted on the surface.

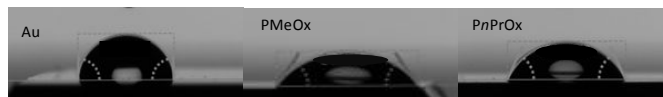


Figure 9 Wettability of, a) Au surface, b) Au modified by PMeOx, c) Au modified by PnPrOx

Finally, PMeOx was also grafted on arrays of gold triangle deposited by nanosphere lithography on ITO. SEM image of such substrates are given as **Figure S7**. These substrates show localized surface plasmon resonance (LSPR) at 800 nm. The wavelength of such LSPR is known to be highly sensitive to the surrounding medium with a red shift when an organic material with dielectric constant above 1 is deposited on the nanotriangles. **Figure S8** shows that upon PMeOx electrografting the LSPR of the gold nanotriangle red shift from 824 nm to 854 nm which again clearly demonstrates that an organic layer has been deposited on the gold Nps.^{20,62}

In summary, several poly(2-oxazoline)s bearing an aminophenyl end group were synthesized by cationic ring-opening polymerization and carefully characterized. The electrografting of these polymers in acetonitrile solution on indium tin oxide (ITO), gold (Au), through a two-dimensional poly(styrene) (PS) template or on ITO bearing gold nanotriangles (AuNPs) were demonstrated. On all substrates, ultrathin layers of polymer are obtained. Nanoporous honeycomb POx structures have been obtained thanks to the electrochemical growth in the interstitial spaces between self-assembled PS sphere. The effect of POx grafting on the plasmonic properties of AuNPs was reported and the wettability of the surfaces was shown to markedly depends on the chemical nature of the POx. On a more general point of view this study demonstrates that surfaces modified by poly(2-oxazoline) can be easily obtained which could be of tremendous interest in order to replace PEO coatings for various applications using biocompatible surfaces.

EXPERIMENTAL SECTION

1. Materials

2-methyl-2-oxazoline (98%, Aldrich), 2-*n*-propyl-2-oxazoline (98%, TCI), allyl bromide (97%, Aldrich) and acetonitrile (VWR) were dried over CaH₂ before use. 1-(4-aminophenyl)piperazine (97%, Aldrich) and N-dimethylformamide (anhydrous, 99.8%, Aldrich), methanol

were used without further purification. Deuterated chloroform was purchased from Euriso-TOP. Dialysis membranes used were Biotech Cellulose Ester membranes with a 500 Da cutoff pore size (Spectrum Labs).

2. Instruments

NMR spectroscopy

^1H and ^{13}C NMR analyses were performed on a Bruker Avance 300 or 400 MHz spectrometer. All spectra are internally referenced to residual proton signals of the deuterated solvent (CDCl_3). The Diffusion-Ordered Spectroscopy (DOSY) experiments were carried out at 298 K on a 400 MHz spectrometer using the ledbgp2s.mod pulse sequence with a linear gradient of 16 steps between 5% and 95%. The maximum field gradient strength was equal to $5.54 \text{ G}\cdot\text{mm}^{-1}$. Before each diffusion experiment, the length of the gradient δ and the diffusion time Δ were optimized. The software used for data analysis was Topspin. The used mathematical treatment of the data was previously described.⁶³

Size Exclusion Chromatography (SEC)

Polymer molar masses were determined by SEC using DMF (containing $1 \text{ g}\cdot\text{L}^{-1}$ lithium bromide). The analyses were performed at 60°C , and at a flow rate of $0.8 \text{ mL}\cdot\text{min}^{-1}$, at a polymer concentration of $5 \text{ mg}\cdot\text{mL}^{-1}$ after filtration through $0.22 \mu\text{m}$. The steric exclusion was carried out on two PSS GRAM 1000 Å columns ($8 \times 300 \text{ mm}$; separation limits: $1\text{--}1000 \text{ kg}\cdot\text{mol}^{-1}$) and one PSS GRAM 30 Å ($8 \times 300 \text{ mm}$; separation limits: $0.1\text{--}10 \text{ kg}\cdot\text{mol}^{-1}$) coupled with three detectors (Viscotek, TDA 305), a differential refractive index (RI) detector and an UV detector). The OmniSEC 4.6.2 software was used for data acquisition and data analysis. The number-average molar masses (M_n), the weight-average molar masses (M_w), and dispersity ($\mathcal{D}=M_w/M_n$) were determined with a calibration curve based on narrow poly(methyl methacrylate) (PMMA) standards (from Polymer Standard Services), using the RI detector.

Nano DSC

Thermograms were measured using a N-DSC III instrument from TA Instruments. The reference cell was filled with water and the sample cell (0.3 mL) with the polymer solution. The capillary cells were not capped, and a constant pressure of 6.10^5 Pa was applied. A baseline scan (solvent in both reference and sample cells) was systematically performed in identical conditions and subtracted from the sample scan. Transition temperature was measured as the average of heating and cooling scans, at a scan rate of $1^\circ\text{C}/\text{min}$.

XPS analysis

XPS analysis was performed using Kratos AXIS XPS with Al K α radiation and depth profiling with a 4 kV Ar^+ beam at 5.10^{-10} Torr. Deposition of PMeOx and PnPrOx layer was achieved using the same procedure as that for cited before. Survey and high-resolution spectra for C, N, O, and Au were obtained initially and after polymers grafting. CasaXPS software was used for deconvolution of the XPS spectra using a Shirley baseline and Gaussian-Lorentzian line shapes.

Atomic Force Microscopy (AFM) and Scanning Electron Microscopy (SEM)

AFM experiments were carried out in the tapping mode. Silicon AFM probes (Tap300-G), with a stiffness constant of 40 Nm^{-1} and a resonance frequency of 300 kHz , were used. SEM experiments were carried out using a Zeiss supra 40 apparatus.

Localized Surface Plasmon Resonance (LSPR) Extinction measurements were carried out with an Ocean Optics HR 4000 UV-vis spectrophotometer (optical resolution: 0.3 nm) coupled with a fiber-optic system which made it possible to analyze an area of $80 \mu\text{m} \times 80 \mu\text{m}$.

3. Polymerizations of 2-methyl-2-oxazoline and 2-n-propyl-2-oxazoline. PMeOx and PnPrOx were synthesized via cationic ring-opening polymerization using the same operating conditions: polymerizations were carried in acetonitrile (ACN) at 80°C under nitrogen and the initial monomer concentration was set to $1.5 \text{ mol}\cdot\text{L}^{-1}$. The procedure was detailed for run 2 of Table 1. In a glove box under a nitrogen atmosphere, $20 \mu\text{L}$ ($2.31\cdot 10^{-4}$ mole, 1 eq) of allyl bromide, 7.4 mL of ACN and 1.08 mL ($1.27\cdot 10^{-2}$ mol, 55 eq) of MeOx were successively introduced a schlenk flask equipped with a magnetic stirrer. The polymerization was stirred at 80°C for 24 h, then quenched at room temperature by adding an excess of 1-(4-aminophenyl)piperazine (205 mg, $1.16\cdot 10^{-3}$ mole, 5 eq, dissolved in 3 mL of ACN). The mixture was stirred for 66h. The solvent was then evaporated and the polymer was dried in vacuum overnight at 50°C , yielding a solid product. This product was solubilized in methanol and dialyzed against methanol for 8h to remove the quencher excess. The monomer conversion was determined from reaction medium before the solvent elimination by ^1H NMR spectroscopy, while molar masses were determined from purified polymer by SEC and ^1H NMR.

4. Elaboration of the Polystyrene Nanosphere Mask Monodisperse carboxyl-terminated polystyrene (PS) spheres with diameters (D) of 500 nm were purchased from MicroParticles GmbH as $10 \text{ wt}\%$ or $5 \text{ wt}\%$ suspensions in water. Self-assembled PS masks were formed on GC or ITO surfaces as follows: the suspension of PS spheres was first diluted in ethanol/Milli-Q water (1:1) in order to obtain a $2.5 \text{ wt}\%$ suspension. Then a 10 mL droplet of the dilution was spread onto a glass microscope slide, which was tilted by 45° into a glass crystallizing dish containing 30 mL of Milli-Q water and 10 mL of a $2 \text{ wt}\%$ solution of sodium dodecyl sulfate (SDS) in water. The PS spheres slid down onto the water surface, where they formed a close-packed monolayer after a few minutes. In a final step, this stable film of PS spheres was slowly transferred onto a clean hydrophilic GC or ITO substrate (the substrates were made hydrophilic by sonication for 1 h. in a $\text{H}_2\text{O}:\text{NH}_4\text{OH}:\text{H}_2\text{O}_2$ (5:1:1 v/v) cleaning solution). Monolayers of quasi-perfect hexagonally close-packed PS spheres with areas up to a few square centimeters were easily obtained. Before using these substrates for electrografting of the organic layer, they were rinsed with large amounts of Milli-Q water with stirring for 2 h. at 60°C in order to reduce the concentration of SDS at the surface.

5. Electrografting of the Organic Layer

The grafting of the organic layer was performed by cyclic voltammetry (CV) using a conventional three-electrode electrochemical system. A saturated calomel electrode (SCE) was used as the reference electrode and the counter-electrode was a stainless steel mesh. The previously synthesized, PMeOx and PnPrOx, was dissolved in acetonitrile at a concentration of $5\cdot 10^{-4} \text{ M}$, and the diazonium salt was generated in situ by adding 20 eq. of *tert*-butylnitrite.⁶⁴ Grafting was performed by successive potential sweeps from 0.45 to $-0.8 \text{ V}/\text{SCE}$ at a scan rate of 100 mVs^{-1} , leading to a PMeOx film around the PS spheres. Finally, the PS spheres were removed by immersing the electrode in tetrahydrofuran for 24 h.

ASSOCIATED CONTENT

Supporting Information. 2D NMR analyses (COSY, HSQC and DOSY NMR, Size Exclusion Chromatography (SEC) of the generated polymers, SEM image of a plasmonic electrode bearing gold nanotriangles deposited by nanosphere lithography, Extinction spectra of the plasmonic electrode before and after PMeOx electrochemical grafting.

AUTHOR INFORMATION

Corresponding Author

* E-mail:

lacroix@univ-paris-diderot.fr

Philippe.guegan@sorbonne-universite.fr

ORCID

Lacroix jean christophe [0000-0002-7024-4452](https://orcid.org/0000-0002-7024-4452)

Guégan Philippe : 0000-0002-4919-0779

Nguyen Van Quynh : 0000-0002-1860-4385

Bennevault Véronique : 0000-0001-6653-3270

Martin Pascal : 0000-0003-1010-8421

Author Contributions

All authors have given approval to the final version of the manuscript.

Funding Sources

AANR (Agence Nationale de la Recherche) and CGI (Commissariat à l'Investissement d'Avenir) are gratefully acknowledged for their financial support of this work through Labex SEAM (Science and Engineering for Advanced Materials and devices) ANR 11 LABX 086, ANR 11 IDEX 05 02

Notes

The authors declare no competing financial interest.

ABBREVIATIONS

Poly(2-oxazoline) = POx

Poly(2-methyl-2-oxazoline) = PMeOx

Poly(*n*-propyl-2-oxazoline) = PnPrOx

Indium tin oxide = ITO

Tetrahydrofuran = THF

Gold nanoparticles = AuNPs

Scanning electron microscopy = SEM

X-ray photoelectron spectroscopy = XPS

Atomic force microscopy = AFM

Contact angle = CA

Cyclic voltammogram = CV

Localized Surface Plasmon Resonance = LSPR

REFERENCES

- (1) Wang, D.; Bierwagen, G. P. Sol-Gel Coatings on Metals for Corrosion Protection. *Prog. Org. Coatings* **2009**, *64* (4), 327–338.
- (2) Montemor, M. F. Functional and Smart Coatings for Corrosion Protection: A Review of Recent Advances. *Surf. Coatings Technol.* **2014**, *258*, 17–37.
- (3) Santos, L.; Martin, P.; Ghilane, J.; Lacaze, P.; Lacroix, J.-C. Micro/Nano-Structured Polypyrrole Surfaces on

Oxidizable Metals as Smart Electroswitchable Coatings. *ACS Appl. Mater. Interfaces* **5** (20), 10159–10164.

- (4) Nath, N.; Chilkoti, A. Creating “Smart” Surfaces Using Stimuli Responsive Polymers. *Adv. Mater.* **2002**, *14* (17), 1243–1247.
- (5) Xia, F.; Zhu, Y.; Feng, L.; Jiang, L. Smart Responsive Surfaces Switching Reversibly between Super-Hydrophobicity and Super-Hydrophilicity. *Soft Matter* **2009**, *5* (2), 275–281.
- (6) Nguyen, V.-Q.; Schaming, D.; Martin, P.; Lacroix, J.-C. Highly Resolved Nanostructured PEDOT on Large Areas by Nanosphere Lithography and Electrodeposition. *ACS Appl. Mater. Interfaces* **2015**, *7* (39), 21673–21681.
- (7) Stuart, M. A. C.; Huck, W. T. S.; Genzer, J.; Müller, M.; Ober, C.; Stamm, M.; Sukhorukov, G. B.; Szleifer, I.; Tsukruk, V. V.; Urban, M.; et al. Emerging Applications of Stimuli-Responsive Polymer Materials. *Nat. Mater.* **2010**, *9* (2), 101–113.
- (8) Wei, T.; Tang, Z.; Yu, Q.; Chen, H. Smart Antibacterial Surfaces with Switchable Bacteria-Killing and Bacteria-Releasing Capabilities. *ACS Appl. Mater. Interfaces* **2017**, *9* (43), 37511–37523.
- (9) Slowing, I.; Trewyn, B. G.; Lin, V. S.-Y. Effect of Surface Functionalization of MCM-41-Type Mesoporous Silica Nanoparticles on the Endocytosis by Human Cancer Cells. *J. Am. Chem. Soc.* **2006**, *128* (46), 14792–14793.
- (10) Pelaz, B.; Del Pino, P.; Maffre, P.; Hartmann, R.; Gallego, M.; Rivera-Fernández, S.; De La Fuente, J. M.; Nienhaus, G. U.; Parak, W. J. Surface Functionalization of Nanoparticles with Polyethylene Glycol: Effects on Protein Adsorption and Cellular Uptake. *ACS Nano* **2015**, *9* (7), 6996–7008.
- (11) Love, J. C.; Estroff, L. A.; Kriebel, J. K.; Nuzzo, R. G.; Whitesides, G. M. Self-Assembled Monolayers of Thiolates on Metals as a Form of Nanotechnology. *Chem. Rev.* **2005**, *105* (4), 1103–1169.
- (12) Ruckenstein, E.; Li, Z. F. Surface Modification and Functionalization through the Self-Assembled Monolayer and Graft Polymerization. *Adv. Colloid Interface Sci.* **2005**, *113* (1), 43–63.
- (13) Everett, W. R.; Fritsch-Faules, I. Factors That Influence the Stability of Self-Assembled Organothiols on Gold under Electrochemical Conditions. *Anal. Chim. Acta* **1995**, *307* (2), 253–268.
- (14) Allara, D. L.; Parikh, A. N.; Rondelez, F. Evidence for a Unique Chain Organization in Long Chain Silane Monolayers Deposited on Two Widely Different Solid Substrates. *Langmuir* **1995**, *11* (7), 2357–2360.
- (15) Soler-Illia, G. J. D. A. A.; Sanchez, C.; Lebeau, B.; Patarin, J. Chemical Strategies to Design Textured Materials: From Microporous and Mesoporous Oxides to Nanonetworks and Hierarchical Structures. *Chem. Rev.* **2002**, *102* (11), 4093–4138.
- (16) Pinson, J.; Podvorica, F. Attachment of Organic Layers to Conductive or Semiconductive Surfaces by Reduction of Diazonium Salts. *Chem. Soc. Rev.* **2005**, *34* (5), 429–439.
- (17) Bélanger, D.; Pinson, J. Electrografting: A Powerful Method for Surface Modification. *Chem. Soc. Rev.* **2011**, *40* (7), 3995.
- (18) Bahr, J. L.; Yang, J.; Kosynkin, D. V.; Bronikowski, M. J.; Smalley, R. E.; Tour, J. M. Functionalization of Carbon Nanotubes by Electrochemical Reduction of Aryl

- Diazonium Salts: A Bucky Paper Electrode. *J. Am. Chem. Soc.* **2001**, *123* (27), 6536–6542.
- (19) Bouriga, M.; Chehimi, M. M.; Combellas, C.; Decorse, P.; Kanoufi, F.; Deronzier, A.; Pinson, J. Sensitized Photografting of Diazonium Salts by Visible Light. *Chem. Mater.* **2013**, *25* (1), 90–97.
- (20) Nguyen, V. Q.; Ai, Y.; Martin, P.; Lacroix, J. C. Plasmon-Induced Nanolocalized Reduction of Diazonium Salts. *ACS Omega* **2017**, *2* (5), 1947–1955.
- (21) Bastide, M.; Gam-Derouich, S.; Lacroix, J.-C. Long-Range Plasmon-Induced Anisotropic Growth of an Organic Semiconductor between Isotropic Gold Nanoparticles. *Nano Lett.* **2022**.
- (22) Adenier, A.; Combellas, C.; Kanoufi, F.; Pinson, J.; Podvorica, F. I. Formation of Polyphenylene Films on Metal Electrodes by Electrochemical Reduction of Benzenediazonium Salts. *Chem. Mater.* **2006**, *18* (8), 2021–2029.
- (23) Nguyen, V.-Q.; Schaming, D.; Martin, P.; Lacroix, J.-C. Nanostructured Mixed Layers of Organic Materials Obtained by Nanosphere Lithography and Electrochemical Reduction of Aryldiazonium Salts. *Langmuir* **2019**, *35* (47), 15071–15077.
- (24) Santos, L.; Ghilane, J.; Lacroix, J. C. Formation of Mixed Organic Layers by Stepwise Electrochemical Reduction of Diazonium Compounds. *J. Am. Chem. Soc.* **2012**, *134* (12), 5476–5479.
- (25) Bousquet, A.; Ceccato, M.; Hinge, M.; Pedersen, S. U.; Daasbjerg, K. Redox Grafting of Diazotated Anthraquinone as a Means of Forming Thick Conducting Organic Films. *Langmuir* **2011**, *28* (2), 1267–1275.
- (26) Nguyen, Q. V.; Martin, P.; Frath, D.; Luisa Della Rocca, M.; Lajolet, F.; Bellinck, S.; Lafarge, P.; Lacroix, J.-C. Highly Efficient Long-Range Electron Transport in a Viologen-Based Molecular Junction. *J. Am. Chem. Soc.* **2018**, *140* (32), 10131–10134.
- (27) Joussemme, B.; Bidan, G.; Billon, M.; Goyer, C.; Kervella, Y.; Guillerez, S.; Hamad, E. A.; Goze-Bac, C.; Mevellec, J.-Y. Y.; Lefrant, S. One-Step Electrochemical Modification of Carbon Nanotubes by Ruthenium Complexes via New Diazonium Salts. *J. Electroanal. Chem.* **2008**, *621* (2), 277–285.
- (28) Combellas, C.; Kanoufi, F.; Pinson, J.; Podvorica, F. I. Sterically Hindered Diazonium Salts for the Grafting of a Monolayer on Metals. *J. Am. Chem. Soc.* **2008**, *130* (27), 8576–8577.
- (29) Nguyen, V. Q.; Sun, X.; Lajolet, F.; Audibert, J. F.; Miomandre, F.; Lemerrier, G.; Loiseau, F.; Lacroix, J. C. Unprecedented Self-Organized Monolayer of a Ru(II) Complex by Diazonium Electroreduction. *J. Am. Chem. Soc.* **2016**, *138* (30), 9381–9384.
- (30) Frath, D.; Nguyen, V. Q.; Lajolet, F.; Martin, P.; Lacroix, J.-C. Electrografted Monolayer Based on a Naphthalene Diimide–Ruthenium Terpyridine Complex Dyad: Efficient Creation of Large-Area Molecular Junctions with High Current Densities. *Chem. Commun.* **2017**, *53* (80), 10997–11000.
- (31) Leroux, Y. R.; Fei, H.; Noël, J.-M.; Roux, C.; Hapiot, P. Efficient Covalent Modification of a Carbon Surface: Use of a Silyl Protecting Group To Form an Active Monolayer. *J. Am. Chem. Soc.* **2010**, *132* (40), 14039–14041.
- (32) Fontaine, O.; Ghilane, J.; Martin, P.; Lacroix, J.-C.; Randriamahazaka, H. Ionic Liquid Viscosity Effects on the Functionalization of Electrode Material through the Electroreduction of Diazonium. *Langmuir* **26** (23), 18542–18549.
- (33) Menanteau, T.; Levillain, E.; Breton, T. Electrografting via Diazonium Chemistry: From Multilayer to Monolayer Using Radical Scavenger. *Chem. Mater.* **2013**, *25* (14), 2905–2909.
- (34) Breton, T.; Downard, A. J. Controlling Grafting from Aryldiazonium Salts: A Review of Methods for the Preparation of Monolayers. *Aust. J. Chem.* **2017**, *70* (9), 960–972.
- (35) Pichereau, L.; López, I.; Cesbron, M.; Dabos-Seignon, S.; Gautier, C.; Breton, T. Controlled Diazonium Electrografting Driven by Overpotential Reduction: A General Strategy to Prepare Ultrathin Layers. *Chem. Commun.* **2019**, *55* (4), 455–457.
- (36) Milner, S. T. Polymer Brushes. *Science* (80-.). **1991**, *251* (4996), 905–914.
- (37) Barbey, R.; Lavanant, L.; Paripovic, D.; Schuwer, N.; Sugnaux, C.; Tugulu, S.; Klok, H.-A. Polymer Brushes via Surface-Initiated Controlled Radical Polymerization: Synthesis, Characterization, Properties, and Applications. *Chem. Rev.* **2009**, *109* (11), 5437–5527.
- (38) Edmondson, S.; Osborne, V. L.; Huck, W. T. S. Polymer Brushes via Surface-Initiated Polymerizations. *Chem. Soc. Rev.* **2004**, *33* (1), 14–22.
- (39) Mahouche-Chergui, S.; Gam-Derouich, S.; Mangeney, C.; Chehimi, M. M. Aryl Diazonium Salts: A New Class of Coupling Agents for Bonding Polymers, Biomacromolecules and Nanoparticles to Surfaces. *Chem. Soc. Rev.* **2011**, *40* (7), 4143–4166.
- (40) Gam-Derouich, S.; Ngoc Nguyen, M.; Madani, A.; Maouche, N.; Lang, P.; Perruchot, C.; Chehimi, M. M. Aryl Diazonium Salt Surface Chemistry and ATRP for the Preparation of Molecularly Imprinted Polymer Grafts on Gold Substrates. *Surf. Interface Anal.* **2010**, *42* (6-7), 1050–1056.
- (41) Gam-Derouich, S.; Carbonnier, B.; Turmine, M.; Lang, P.; Jouini, M.; Ben Hassen-Chehimi, D.; M. Chehimi, M. Electrografted Aryl Diazonium Initiators for Surface-Confining Photopolymerization: A New Approach to Designing Functional Polymer Coatings. *Langmuir* **2010**, *26* (14), 11830–11840.
- (42) Gam-Derouich, S.; Mahouche-Chergui, S.; Turmine, M.; Piquemal, J.-Y.; Hassen-Chehimi, D. Ben; Omastová, M.; Chehimi, M. M. A Versatile Route for Surface Modification of Carbon, Metals and Semi-Conductors by Diazonium Salt-Initiated Photopolymerization. *Surf. Sci.* **2011**, *605* (21–22), 1889–1899.
- (43) Adenier, A.; Cabet-Deliry, E.; Lalot, T.; Pinson, J.; Podvorica, F. Attachment of Polymers to Organic Moieties Covalently Bonded to Iron Surfaces. *Chem. Mater.* **2002**, *14* (11), 4576–4585.
- (44) Mahouche, S.; Mekni, N.; Abbassi, L.; Lang, P.; Perruchot, C.; Jouini, M.; Mammari, F.; Turmine, M.; Romdhane, H. Ben; Chehimi, M. M. Tandem Diazonium Salt Electroreduction and Click Chemistry as a Novel, Efficient Route for Grafting Macromolecules to Gold Surface. *Surf. Sci.* **2009**, *603* (21), 3205–3211.
- (45) Squillace, O.; Esnault, C.; Pilard, J.-F.; Brotons, G. Grafting Commercial Surfactants (Brij, CiEj) and PEG to Electrodes via Aryldiazonium Salts. *ACS Appl. Mater. Interfaces* **2017**, *9* (48), 42313–42326.
- (46) Romero-Ben, E.; Cid, J. J.; Assali, M.; Fernández-García,

- E.; Wellinger, R. E.; Khiar, N. Surface Modulation of Single-Walled Carbon Nanotubes for Selective Bacterial Cell Agglutination. *Int. J. Nanomedicine* **2019**, *14*, 3245–3263.
- (47) Du, H.; de Oliveira, F. A.; Albuquerque, L. J. C.; Tresset, G.; Pavlova, E.; Huin, C.; Guégan, P.; Giacomelli, F. C. Polyglycidol-Stabilized Nanoparticles as a Promising Alternative to Nanoparticle PEGylation: Polymer Synthesis and Protein Fouling Considerations. *Langmuir* **2020**, *36* (5), 1266–1278.
- (48) Le, D.; Wagner, F.; Takamiya, M.; Hsiao, I.L.; Alvadero, G.G.; Sträle, U.; Weiss, C.; Delaitre, G. Straightforward access to biocompatible poly(2-oxazoline)-coated nanomaterials by polymerization-induced self-assembly *Chem. Commun.*, **2019**, 3741–3744.
- (49) Morgese, G.; Benetti, E.M; Polyoxazoline biointerfaces by surface grafting *Eur. Pol. J.* **2017** *88*, 470–485.
- (50) Jordan, R.; Ulman, A. Surface Initiated Living Cationic Polymerization of 2-Oxazolines. *J. Am. Chem. Soc.* **1998**, *120* (2), 243–247.
- (51) Jordan, R.; West, N.; Ulman, A.; Chou, Y.-M.; Nuyken, O. Nanocomposites by Surface-Initiated Living Cationic Polymerization of 2-Oxazolines on Functionalized Gold Nanoparticles. *Macromolecules* **2001**, *34* (6), 1606–1611.
- (52) Trachsel, L.; Romio, M.; Grob, B.; Zenobi-Wong, M.; Spencer, N. D.; Ramakrishna, S. N.; Benetti, E. M. Functional Nanoassemblies of Cyclic Polymers Show Amplified Responsiveness and Enhanced Protein-Binding Ability. *ACS Nano* **2020**, *14* (8), 10054–10067.
- (53) Yan, W.; Divandari, M.; Rosenboom, J.-G.; Ramakrishna, S. N.; Trachsel, L.; Spencer, N. D.; Morgese, G.; Benetti, E. M. Design and Characterization of Ultrastable, Biopassive and Lubricious Cyclic Poly(2-Alkyl-2-Oxazoline) Brushes. *Polym. Chem.* **2018**, *9* (19), 2580–2589.
- (54) Waqas Ali, M.; Muhammad, Z.; Jia, Q.; Li, L.; Saleem, M., Siddiq, M.; Chen, Y. Synthesis of cyclic poly(2-ethyl-2-oxazoline) with a degradable disulfide bond *Polym. Chem.*, **2020**, *11*, 4164–4171.
- (55) Plet, L.; Delecourt, G.; Hanafi, M.; Pantoustier, N.; Pouembong, G.; Midoux, P.; Bennevault, V.; Guégan, P. Controlled star poly(2-oxazoline)s: Synthesis, characterization *Eur. Pol. J.* **2020** *122*, , 109323.
- (56) Delecourt, G.; Plet, L.; Bennevault, V.; Guégan, P. Synthesis of double hydrophilic block copolymers poly(2-oxazoline-*b*-ethylenimine) in two steps procedure *ACS Appl. Polym. Mater.* **2020** *2* (7), 2696–2705.
- (57) Hoogenboom, R.; Thijs, H.M.L.; Jochems, M.J.H.C.; van Lankvelt, B.M.; Fijten, M.W.M. Schubert, U.S. Tuning the LCST of poly(2-oxazoline)s by varying composition and molecular weight: alternatives to poly(*N*-isopropylacrylamide)? *Chem. Comm.* **2008**, 5758–5760.
- (58) Hoogenboom, R. Poly(2-oxazoline)s: Alive and Kicking *Macromol. Chem Phys.* **2007**, *208*(1), 18–25.
- (59) Baranton, S.; Bélanger, D. In Situ Generation of Diazonium Cations in Organic Electrolyte for Electrochemical Modification of Electrode Surface. *Electrochim. Acta* **2008**, *53* (23), 6961–6967.
- (60) Santos, L.; Ghilane, J.; Lacroix, J.-C. Surface Patterning Based on Nanosphere Lithography and Electroreduction of in Situ Generated Diazonium Cation. *Electrochem. commun.* **2012**, *18*, 20–23.
- (61) Nguyen, V.-Q.; Schaming, D.; Tran, D. L.; Lacroix, J.-C. Ordered Nanoporous Thin Films by Nanosphere Lithography and Diazonium Electroreduction: Simple Elaboration of Ultra-Micro-Electrode Arrays. *ChemElectroChem* **2016**, *3* (12), 2264–2269.
- (62) Schaming, D.; Nguyen, V.-Q.; Martin, P.; Lacroix, J.-C. Tunable Plasmon Resonance of Gold Nanoparticles Functionalized by Electroactive Bisthienylbenzene Oligomers or Polythiophene. *J. Phys. Chem. C* **2014**, *118* (43), 25158–25166.
- (63) Bennevault-Celton, V.; Urbach, A.; Martin, O.; Pichon, C.; Guégan, P.; Midoux, P. Supramolecular Assemblies of Histidinylated α -Cyclodextrin in the Presence of DNA Scaffold during CDplexes Formation. *Bioconjug. Chem.* **2011**, *22* (12), 2404–2414.
- (64) Stockhausen, V.; Trippe-Allard, G.; Nguyen, V. Q.; Ghilane, J.; Lacroix, J.-C. Grafting π -Conjugated Oligomers Incorporating 3,4-Ethylenedioxythiophene (EDOT) and Thiophene Units on Surfaces by Diazonium Electroreduction. *J. Phys. Chem. C* **2015**, *119* (33), 19218–19227.

(Word Style "TF_References_Section"). References are placed at the end of the manuscript. Authors are responsible for the accuracy and completeness of all references. Examples of the recommended formats for the various reference types can be found at <http://pubs.acs.org/page/4authors/index.html>. Detailed information on reference style can be found in The ACS Style Guide, available from Oxford Press.

Insert Table of Contents artwork here

